

WANG Kai-ge, XIONG Jun, GAO Lu

From Hanbury–Brown and Twiss Experiment to the Second-Order Double-Slit Interference for Incoherent Light

© Higher Education Press and Springer-Verlag 2006

Abstract In this review article, we discuss both experimentally and theoretically the second-order double-slit interference for a thermal light source which is random in transverse propagating direction. We show that when the bandwidth of the noise spectrum is increased, the first-order interference pattern disappears while the sub-wavelength pattern fringe emerges in the intensity correlation measurement. Our theoretical description, which is carried out in contrast with coherent light and two-photon state sources, demonstrates that this effect can be explained in accordance with the Hanbury–Brown and Twiss experiment.

Keywords Hanbury-Brown and Twiss effect, subwavelength interference, two-photon entanglement

PACS numbers 42.50.Dv, 42.50.St, 42.25.Hz

1 Introduction

Double-slit interference is a perpetual subject in physics. Since the first double-slit experiment was originally performed by the physicist and physician Thomas Young around 1805, the debate was resolved whether light was composed of particles (the “corpuscular” theory), or consisted of waves travelling through some aether. A century later, the new debate about wave-like and particle-like was aroused when the quantum phenomena were discovered. Single-photon interference through a double slit is one of the defining experiments of quantum mechanics, and there is no other simple experiment that demonstrates the wave-particle duality so well. This led to Dirac’s famous statement that “each

photon then interferes only with itself”. Furthermore, the double-slit interference is an important experimental evidence of the de Broglie wave for matter. Richard Feynman described the double-slit interference for particles as “a phenomenon which is impossible, absolutely impossible, to explain in any classical way, and which has in it the heart of quantum mechanics. In reality it contains only mystery” [1]. In frequent discussions about quantum theory, however, the double-slit interference acts as a classic Gedanken experiment (thought experiment) for its clarity in expressing the central puzzles of quantum mechanics.

In the 1960s, when laser was invented and the coherence theory of optical field was established, the double-slit interference pattern was the sign and measure of the spatial coherence of the light source. For a coherent source, where all the atoms radiate cooperatively such as a laser, the double-slit interference pattern can be easily observed with perfect visibility. However, for an incoherent source, where atoms radiate independently, the spatial coherence is limited by the van Cittert–Zernike theorem [2], and the double-slit interference does not occur when the dimension of the source is out of the coherent area. The physical reason is quite intuitional: in the incoherent source, the independent rays randomly propagating along different directions form the fringes at different positions and, as a result, their incoherent superposition degrades the fringe. One might conclude that the disorder in propagating directions for the incoherent source destroys the coherent information completely. We will see that this is not true.

The above discussion concerns only the first-order (or one-photon) double-slit interference where the one-photon intensity distribution $\langle E^{(-)}(x)E^{(+)}(x) \rangle$ in the detection plane is measured. Since the 1980s, some peculiar quantum phenomena of two-photon entanglement have drawn much interest. Among them, two-photon coincidence (or ghost) imaging/interference [3–13] and sub-wavelength interference [14–25] were extensively studied both experimentally and theoretically. The original idea of these schemes was proposed by Klyshko [26]. In observation of these effects, a two-photon coincidence measurement and a two-photon absorption detection are performed to evaluate the second-

WANG Kai-ge (✉), XIONG Jun, GAO Lu
Department of Physics,
Applied Optics Beijing Area Major Laboratory,
Beijing Normal University,
Beijing 100875, China
E-mail: wangkg@bnu.edu.cn

WANG Kai-ge
The Abdus Salam International Centre for Theoretical Physics,
34014 Trieste, Italy

order correlation functions $\langle E^{(-)}(x_1)E^{(+)}(x_1)E^{(-)}(x_2)E^{(+)}(x_2) \rangle$ and $\langle E^{(-)}(x)E^{(-)}(x)E^{(+)}(x)E^{(+)}(x) \rangle$, respectively. Since these effects had indeed never been observed in classical optics before, they are nominated with an unusual word “ghost”. In particular, sub-wavelength interference was regarded as a non-classical interference that can surpass the Rayleigh diffraction limit and realize the quantum lithography.

Recently, Bennink et al. [27] showed in their experiments that coincidence imaging and coincidence interference can be also performed with a classical light source under certain conditions. A debate was raised if quantum imaging and interference can be classically simulated [28,29]. Further theoretical analyses [30–34] showed that a thermal or quasi-thermal source possesses such a second-order spatial correlation similar to two-photon quantum entanglement, and hence it can perform the correlated imaging/interference and sub-wavelength interference. These effects have been demonstrated in several experiments [35–38].

Indeed, the second-order correlation property of thermal light has been known since Hanbury–Brown and Twiss proposed an optical stellar intensity interferometer in the 1950s [39]. Their work was controversial because it appeared to contradict the established beliefs about quantum interference. It is meaningful that, half a century later, we face again a conflict between quantum entanglement and classical correlation, associated with the Hanbury–Brown and Twiss experiment.

In this article, we review the studies on the second-order double-slit interference for the incoherent light. In Section 2, we describe the experimental observation of the double-slit interference for a pseudo-thermal light source. In Section 3, a simple theoretical explanation to the effect is presented, and the detailed theoretical analysis in terms of the second-order spatial correlation function for coherent field, two-photon entangled state and thermal light is given in Section 4. The summary is shown in the last section.

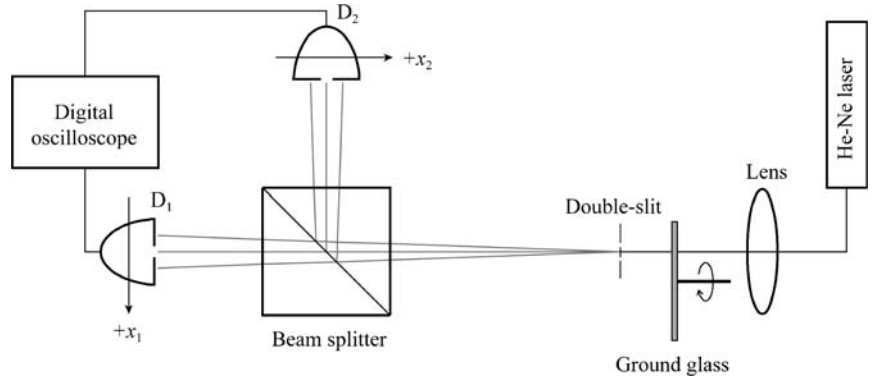
2 Experimental observation

We first review the experimental results obtained by Xiong et al. [35]. The experimental set-up of the second-order double-slit interference for incoherent light shown in Fig. 1 is rather simple and can be performed in an ordinary laboratory. The pseudo-thermal light source is obtained by pass-

ing a focused He–Ne laser beam of wavelength 632.8 nm through a slowly rotating (0.5 Hz) ground glass disk. A double-slit of slits separation $d = 100 \mu\text{m}$ and slit width $b = 55 \mu\text{m}$ is illuminated by the thermal light. For the convenience of simultaneous detection at two positions, the diffracted radiation is split into two beams with a non-polarizing 50/50 beam splitter. The transmitted and reflected beams are detected by small-area (diameter, 0.6 mm) Si photodetectors D_1 and D_2 , which are mounted on translation stages. The signals from the two detectors are recorded on a digital oscilloscope (Tektronics 3012B) for the joint-intensity measurement. By averaging the products of these two signals over a 2-s interval, we obtain the joint-intensity correlation $\langle I_1(x_1)I_2(x_2) \rangle$, where $I_1(x_1)$ and $I_2(x_2)$ are the light intensities detected by D_1 and D_2 at positions x_1 and x_2 , respectively. As a matter of fact, the joint-intensity correlation of the outgoing fields in the beam splitter is proportional to the second-order correlation of the input field. For comparison, we also measured the first-order and second-order interference-diffraction patterns for the coherent light using the same experimental set-up (simply by taking away the glass disk).

The experimental results are plotted in Figs. 2, 3, 4 and 5, where Fig. 2(a), Figs. 3(a)–(c), Fig. 4(a), Fig. 5 show the results for thermal light, and Fig. 2(b), Fig. 3(d) Fig. 4(b) those for coherent light. In Fig. 2, the averaged intensity distributions of the two outgoing beams were individually measured. As expected, the incoherent thermal light produces a diffraction pattern without fringes, whereas the coherent light exhibits the well-known first-order interference fringe. In Figs. 3 and 4, however, we perform the joint-intensity measurement at positions $(x, -x)$ and (x, x) , respectively. (In the experiment, the origin $x = 0$ on the interference screen is not necessarily at the symmetric center of the double-slit, and it can be any position on the screen; see also Section 3.) For the thermal light source, although the intensity observed by each detector exhibits disordered fluctuation, the interference fringes emerge by measuring the normalized joint-intensity correlation $g^{(2)}(x, -x) = \langle I_1(x)I_2(-x) \rangle / [\langle I_1(x) \rangle \langle I_2(-x) \rangle]$, the joint-intensity fluctuation correlation $\Delta G^{(2)}(x, -x) = \langle I_1(x)I_2(-x) \rangle - \langle I_1(x) \rangle \langle I_2(-x) \rangle$ and the joint-intensity correlation $G^{(2)}(x, -x) = \langle I_1(x)I_2(-x) \rangle$, as shown in Fig. 3(a)–(c), respectively. In Fig. 4 (a), the second-order interference disappears in the correlation $g^{(2)}(x, x)$ for the thermal light. For the sake of

Fig. 1 Sketch of the experimental set-up



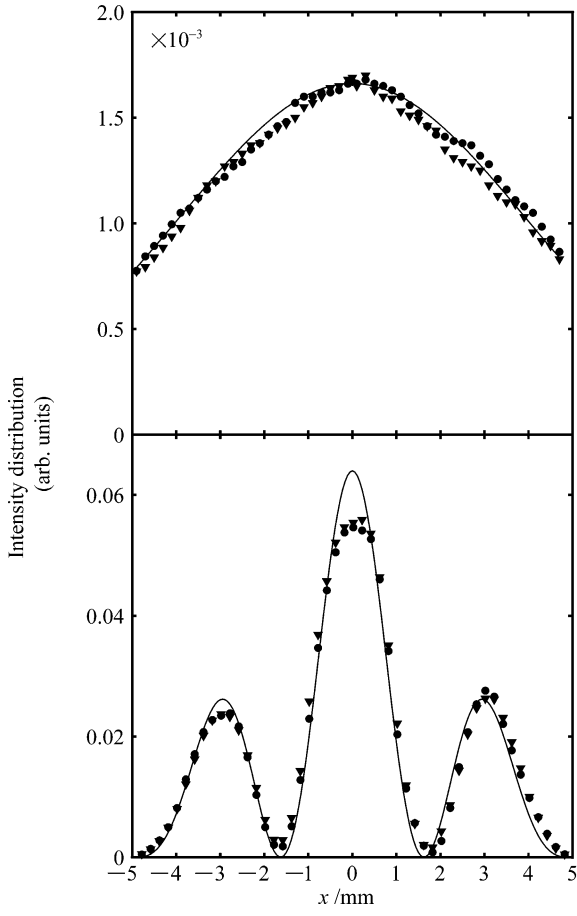


Fig. 2 Average intensity distributions of the two outgoing beams from the beam splitter for (a) the pseudo-thermal light and (b) the coherent light. Experimental data are indicated by *triangles* and *circles* detected by D_1 and D_2 , respectively. In this figure and in Figs. 3, 4 and 5, the *solid lines* represent the numerical simulations

comparison, the measured $G^{(2)}(x,-x)$ and $G^{(2)}(x,x)$ for coherent light are plotted in Figs. 3(d) and 4(b), respectively. It can be seen that the fringe interval for the thermal light is half of that for the laser beam. Furthermore, in Fig. 5, the normalized correlation $g^{(2)}(x,0)$ was measured by fixing one detector and scanning the other detector along x . A similar interference pattern with the same fringe interval as that for the coherent beam is obtained.

The experimental results clearly demonstrate that, for the incoherent light, although the first-order double-slit interference does not exist, the second-order interference does exist.

3 Simple theoretical explanation

3.1 Classical description

The second-order double-slit interference for the incoherent light can be explained in terms of the Hanbury–Brown and Twiss effect. We assume that a monochromatic beam

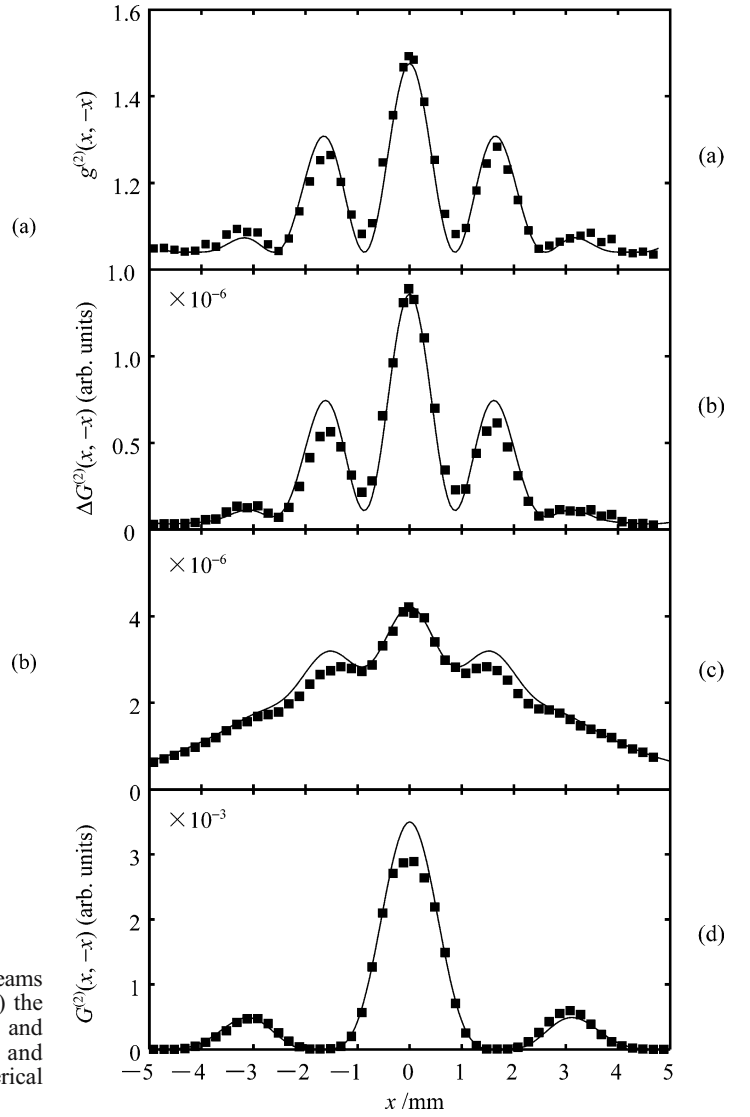


Fig. 3 Interference-diffraction patterns obtained by measuring (a) the normalized joint-intensity correlation function $g^{(2)}(x,-x)$, (b) the joint-intensity correlation fluctuation $\Delta G^{(2)}(x,-x)$ and (c) the joint-intensity correlation $G^{(2)}(x,-x)$ for the pseudo-thermal light. In (d), the function $G^{(2)}(x,-x)$ is measured for coherent light

of wavelength λ illuminates the double-slit, and the fields E_A and E_B at the two slits are completely incoherent, that is, the two fields are statistically independent

$$\langle E_A^* E_B \rangle = \langle E_A^* \rangle \langle E_B \rangle = 0 \quad (1)$$

where $\langle E_A \rangle = \langle E_B \rangle = 0$ is due to the random phase of the fields. As shown in Fig. 6, P_1 and P_2 are two positions on the interference plane. The amplitude and intensity at position P_i ($i = 1, 2$) are obtained as

$$E(P_i) = (1/R)[E_A \exp(ikr_{iA}) + E_B \exp(ikr_{iB})] \quad (i = 1, 2) \quad (2a)$$

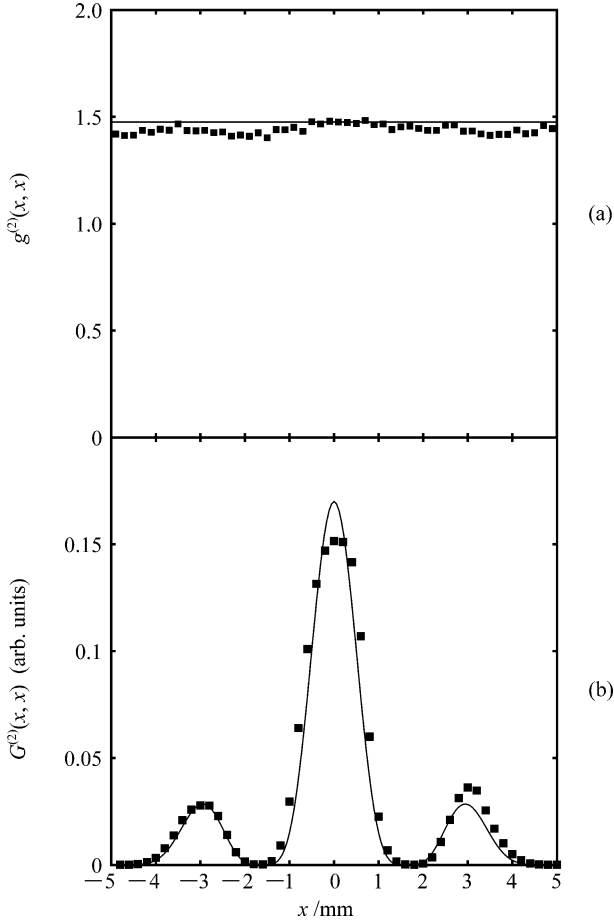


Fig. 4 Interference-diffraction patterns obtained by measuring (a) the normalized joint-intensity correlation function $g^{(2)}(x,x)$ of the pseudo-thermal light, and (b) the joint-intensity correlation function $G^{(2)}(x,x)$ of coherent light

$$I(P_i) = (1/R^2) \left\{ |E_A|^2 + |E_B|^2 + [E_A^* E_B \exp(ikr_i) + \text{c.c.}] \right\} \quad (i = 1, 2) \quad (2b)$$

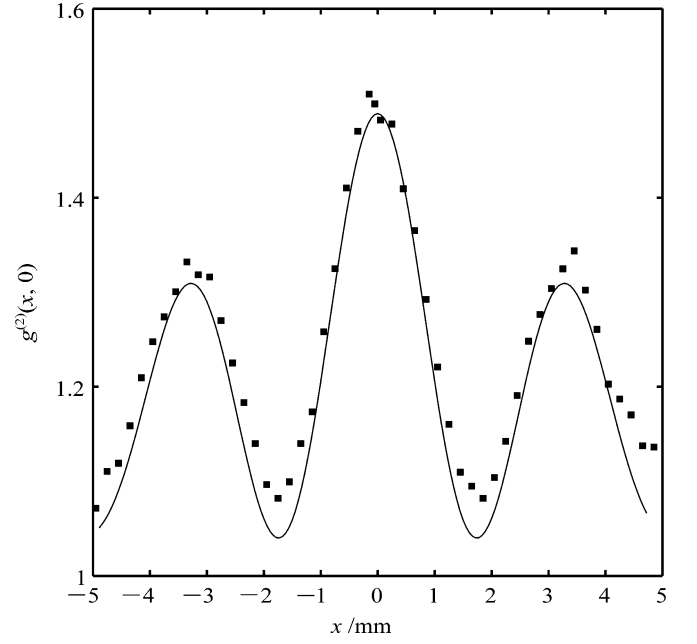


Fig. 5 Interference-diffraction patterns obtained by measuring the normalized joint-intensity correlation function $g^{(2)}(x,0)$ of the pseudo-thermal light

where $k = 2\pi/\lambda$ is the wave number, R is the distance between the slits and the screen, and $r_i \equiv r_{iB} - r_{iA}$ is the path difference from the two slits to position P_i . When the fields at the two slits are incoherent [i.e., Eq. (1)], it is well known that there is no first-order double-slit interference on the observation plane

$$\langle I(P_1) \rangle = \langle I(P_2) \rangle = (1/R^2) (\langle |E_A|^2 \rangle + \langle |E_B|^2 \rangle) \quad (3)$$

We now consider the second-order double-slit interference by the joint-intensity measurement at two positions

$$\begin{aligned} \langle I(P_1)I(P_2) \rangle &= (1/R^4) \left\{ \langle (|E_A|^2 + |E_B|^2)^2 \rangle + \left(\langle (E_A^*)^2 E_A E_B \rangle + \langle E_B^* (E_B)^2 E_A^* \rangle \right) [e^{ikr_1} + e^{ikr_2}] + \text{c.c.} \right. \\ &\quad \left. + \left(\langle (E_A^*)^2 (E_B)^2 \rangle e^{ik(r_1+r_2)} + \text{c.c.} \right) + \langle |E_A|^2 |E_B|^2 \rangle [e^{ik(r_1-r_2)} + \text{c.c.}] \right\} \quad (4) \end{aligned}$$

Taking into account the incoherence of the fields at the two slits, we obtain

$$\begin{aligned} \langle I(P_1)I(P_2) \rangle &= (1/R^4) \left\{ \langle |E_A|^4 \rangle + \langle |E_B|^4 \rangle + 2\langle |E_A|^2 \rangle \langle |E_B|^2 \rangle [1 + \cos k(r_1 - r_2)] \right\} \\ &= (1/R^4) \left\{ \langle |E_A|^4 \rangle + \langle |E_B|^4 \rangle + 2\langle |E_A|^2 \rangle \langle |E_B|^2 \rangle \left[1 + \cos \frac{2\pi d}{\lambda R} (x_1 - x_2) \right] \right\} \quad (5) \end{aligned}$$

where d is the slit interval and $x_i = r_i R/d$ is the transverse coordinate of position P_i . The first two terms introduce a background and the last term displays an interference pattern.

Equation (5) can explain all the experimental results in Section 2. If we scan the two detectors in the opposite direction around any position x_0 , i.e., $x_1 = x_0 + x$ and $x_2 = x_0 - x$, we observe the interference pattern $(1 + \cos \frac{2\pi d}{\lambda R} 2x)$, which shows a half fringe interval of that for the first-order interference (Fig. 3). However, if we scan one detector by fixing the other, we obtain the same interference pattern as the ordinary one (Fig. 5). The interference fringe disappears only when two detectors are scanned in the same direction ($x_1 = x_0 + x$ and $x_2 = x_0 + x$) or a two-photon absorption detector ($x_1 = x_2 = x$) is applied [Fig. 4(a)].

The fringe visibility of the second-order interference can be defined and evaluated as

$$V \equiv \frac{\langle I(P_1)I(P_2) \rangle_{\max} - \langle I(P_1)I(P_2) \rangle_{\min}}{\langle I(P_1)I(P_2) \rangle_{\max} + \langle I(P_1)I(P_2) \rangle_{\min}} \quad (6)$$

$$= \frac{2\langle |E_A|^2 \rangle \langle |E_B|^2 \rangle}{\langle |E_A|^4 \rangle + \langle |E_B|^4 \rangle + 2\langle |E_A|^2 \rangle \langle |E_B|^2 \rangle}$$

If, for example, the fields at the two slits are random only in phase and their intensities are equal without fluctuation, i.e., $|E_A|^2 = |E_B|^2 = I_0$, the fringe visibility is 50%. However, if the source is thermal light satisfying Gaussian statistics, it has $\langle |E|^4 \rangle = 2\langle |E|^2 \rangle^2$ and the visibility is 33.33%.

3.2 Microscopical mechanism

Microscopically, the double-slit interference can be understood in the photon's picture. It is well known that the first-order interference can occur for a single photon. The one-photon state at the double-slit is written as

$$|\Psi\rangle_S = \frac{1}{\sqrt{2}} (a_A^\dagger + a_B^\dagger) |0\rangle \quad (7)$$

in which there is no information about which slit the photon passes through. The field at position P in the detection plane is expressed as

$$E^{(+)}(P) = a_A \exp(ikr_A) + a_B \exp(i) \quad (8)$$

Thus the first-order interference is obtained as

$${}_S \langle \Psi | E^{(-)}(P) E^{(+)}(P) | \Psi \rangle_S = 1 + \cos kr \quad (9)$$

where $r \equiv r_B - r_A = xd/R$ is proportional to the transverse position x in the detection plane (see Fig. 6).

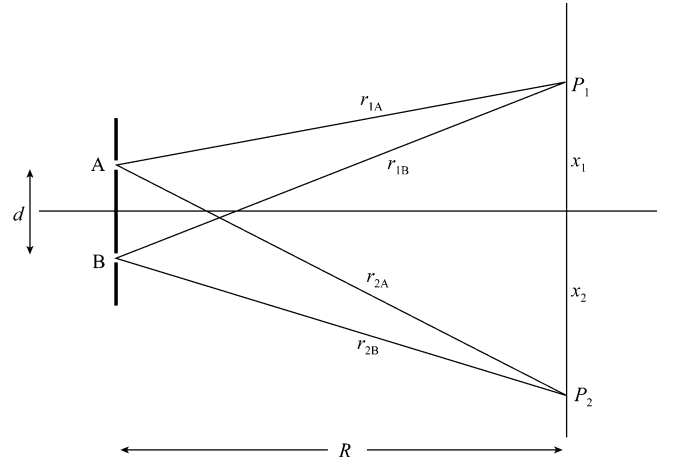


Fig. 6 Sketch of the second-order double-slit interference

In the second-order double-slit interference, however, there are at least two photons involved. We consider three two-photon states at the double slit

$$|\Psi\rangle_{SS} = \frac{1}{\sqrt{8}} (a_A^\dagger + a_B^\dagger) (a_A^\dagger + a_B^\dagger) |0\rangle \quad (10a)$$

$$|\Psi\rangle_{EN} = \frac{1}{2} \left[(a_A^\dagger)^2 + (a_B^\dagger)^2 \right] |0\rangle \quad (10b)$$

$$|\Psi\rangle_{DS} = a_A^\dagger a_B^\dagger |0\rangle \quad (10c)$$

which implicate the ways that two photons pass through the two slits. Both $|\Psi\rangle_{SS}$ and $|\Psi\rangle_{DS}$ describe two independent photons, whereas $|\Psi\rangle_{EN}$ describes the entangled photons. Obviously, $|\Psi\rangle_{SS} = (1/\sqrt{2})(|\Psi\rangle_{EN} + |\Psi\rangle_{DS})$.

The first-order double-slit interference patterns can be evaluated for the three two-photon states

$${}_{SS} \langle \Psi | E^{(-)}(P) E^{(+)}(P) | \Psi \rangle_{SS} = 2(1 + \cos kr) \quad (11a)$$

$${}_{EN} \langle \Psi | E^{(-)}(P) E^{(+)}(P) | \Psi \rangle_{EN} = 2 \quad (11b)$$

$${}_{DS} \langle \Psi | E^{(-)}(P) E^{(+)}(P) | \Psi \rangle_{DS} = 2 \quad (11c)$$

State $|\Psi\rangle_{SS}$ shows the same interference pattern just as the single photon state $|\Psi\rangle_S$, whereas both states $|\Psi\rangle_{EN}$ and $|\Psi\rangle_{DS}$ do not show the first-order interference.

We now consider the second-order interference for these states. In experimental observation, the two-photon coincidence measurement is performed using a beamsplitter. As a result, the second-order correlation of the field at the input port of the beamsplitter is proportional to the two-photon coincidence probability measured at the output ports

$$\begin{aligned} \langle n(P_1)n(P_2) \rangle &\propto \langle E^{(-)}(P_1)E^{(-)}(P_2)E^{(+)}(P_2)E^{(+)}(P_1) \rangle \\ &= |\langle 0|E^{(+)}(P_2)E^{(+)}(P_1)|\Psi \rangle|^2 \end{aligned} \quad (12)$$

where $|\Psi\rangle$ is a two-photon state. We calculate the second-order correlation functions for the three two-photon states

$$\begin{aligned} {}_{SS} \langle \Psi(E^{(-)}(P_1)E^{(-)}(P_2)E^{(+)}(P_2)E^{(+)}(P_1))\Psi \rangle_{SS} \\ = 2(1 + \cos kr_1)(1 + \cos kr_2) \end{aligned} \quad (13a)$$

$$\begin{aligned} {}_{EN} \langle \Psi(E^{(-)}(P_1)E^{(-)}(P_2)E^{(+)}(P_2)E^{(+)}(P_1))\Psi \rangle_{EN} \\ = 2[1 + \cos k(r_1 + r_2)] \end{aligned} \quad (13b)$$

$$\begin{aligned} {}_{DS} \langle \Psi(E^{(-)}(P_1)E^{(-)}(P_2)E^{(+)}(P_2)E^{(+)}(P_1))\Psi \rangle_{DS} \\ = 2[1 + \cos k(r_1 - r_2)] \end{aligned} \quad (13c)$$

which exhibit three types of second-order interference. In state $|\Psi\rangle_{SS}$, the two photons are independent and each of them interferes with itself, so that the second-order interference is the product of two first-order interference patterns. However, both states $|\Psi\rangle_{EN}$ and $|\Psi\rangle_{DS}$ show position correlation in the second-order interference and reveal sub-wavelength interference pattern when $r_1 = r_2$ and $r_1 = -r_2$, respectively. To understand the sub-wavelength interference of the two-photon state $|\Psi\rangle_{EN}$ with respect to the single-photon state $|\Psi\rangle_S$, Jacobson et al. [14] proposed the concept of multi-photon de Broglie wavepacket.

State $|\Psi\rangle_{DS}$ contributes an interference pattern similar to that for the classical incoherent light, as shown in Eq. (5) with the exception of a background. Different from states $|\Psi\rangle_{EN}$ and $|\Psi\rangle_S$, two photons simultaneously pass through the two slits with certainty in state $|\Psi\rangle_{DS}$. But the photon registered by each detector in the coincidence measurement comes from either slit A or slit B, showing uncertainty. Only when the two photons reach the same position $r_1 = r_2$, the uncertainty does not exist and the interference disappears. Although these microscopic states do not mean the macroscopic sources available, the discussions may provide us more intuitive knowledge of interference in the photon's picture.

4 Spatial correlation properties of fields

The above experimental results and theoretical explanation show that the generalized double-slit interference can occur not only for coherent light, but also for incoherent light. This implies that the distinct interference behaviors reflect the spatial correlation properties of fields, rather than the coherence. In this section, we discuss the spatial correlation properties of three sources, a coherent beam, a photon-pair spatially entangled and a thermal light source, and the corresponding interference effects.

The double-slit function $T(x)$ is defined as

$$T(x) = \begin{cases} 1, & x \in \left[-\frac{d+b}{2}, -\frac{d-b}{2}\right] \text{ and } \left[\frac{d-b}{2}, \frac{d+b}{2}\right] \\ 0, & \text{others} \end{cases} \quad (14)$$

where b and d are the width of each slit and the interval between two slits, respectively. An input field $a(x)$ is assumed to be monochromatic. By ignoring the thickness of double-slit, the transverse envelope operators of the input field $a(x)$ and the output field $a_1(x)$ of the double-slit are expressed by

$$a_1(x) = a(x)T(x) + a_v(x)[1 - T(x)] \quad (15)$$

where the vacuum field a_v is introduced for maintaining the bosonic commutation relation. [Note that $T^2(x) = T(x)$.] Since the vacuum field has no contribution to the normal-order correlation, it can be omitted in the calculations below.

We assume that both the double-slit and the detection screen are placed at the two focal planes of a lens of focal length f . In the paraxial approximation, the field $a_2(x)$ in the detection plane is expressed by a Fourier transform of the field at the double-slit $a_1(x)$

$$a_2(x) = \sqrt{\frac{k}{2\pi f}} \int a_1(x') \exp\left[-i\frac{k}{f}x'x\right] dx' \quad (16)$$

Substituting Eq. (15) into Eq. (16), we obtain a convolution

$$a_2(x) = \sqrt{\frac{k}{2\pi f}} \int \tilde{T}\left(\frac{kx}{f} - q\right) a(q) dq \quad (17)$$

where

$$\begin{aligned} \tilde{T}(q) &= \frac{1}{\sqrt{2\pi}} \int T(x) e^{-iqx} dx \\ &= \frac{2b}{\sqrt{2\pi}} \text{sinc}(qb/2) \cos(qd/2) \end{aligned} \quad (18)$$

$\tilde{T}(q)$ and $a(q)$ are the Fourier transforms of $T(x)$ and $a(x)$, respectively, and q is the transverse wavevector. Thus, the

first- and second-order correlation functions in the detection plane are obtained

$$\begin{aligned} G^{(1)}(x_1, x_2) &\equiv \langle a_2^\dagger(x_1)a_2(x_2) \rangle \\ &= \frac{k}{2\pi f} \int \tilde{T}^*\left(\frac{kx_1}{f} - q_1\right) \tilde{T}\left(\frac{kx_2}{f} - q_2\right) \\ &\quad \times \langle a^\dagger(q_1)a(q_2) \rangle dq_1 dq_2 \end{aligned} \quad (19a)$$

$$\begin{aligned} G^{(2)}(x_1, x_2) &\equiv \langle a_2^\dagger(x_1)a_2^\dagger(x_2)a_2(x_2)a_2(x_1) \rangle \\ &= \left(\frac{k}{2\pi f}\right)^2 \int \tilde{T}^*\left(\frac{kx_1}{f} - q_1\right) \\ &\quad \tilde{T}^*\left(\frac{kx_2}{f} - q_2\right) \tilde{T}\left(\frac{kx_2}{f} - q'_2\right) \tilde{T}\left(\frac{kx_1}{f} - q'_1\right) \\ &\quad \langle a^\dagger(q_1)a^\dagger(q_2)a(q'_2)a(q'_1) \rangle dq_1 dq_2 dq'_1 dq'_2 \end{aligned} \quad (19b)$$

$G^{(1)}(x, x)$ and $G^{(2)}(x_1, x_2)$ describe the first- and second-order double-slit interference patterns, respectively. Therefore, the interference patterns reflect the spatial correlation properties of the source field. In the following, we discuss three sources.

4.1 Coherent field source

The coherent state is the border between classical and quantum regimes. We review double-slit interference for a coherent beam, which is assumed to be a monochromatic wave with an angular spectrum $C(q)$, describing the wavefront of the beam. The correlation functions for the coherent field read

$$\langle \alpha | a^\dagger(q_1)a(q_2) | \alpha \rangle = |\alpha|^2 C^*(q_1)C(q_2) \quad (20a)$$

$$\begin{aligned} \langle \alpha | a^\dagger(q_1)a^\dagger(q_2)a(q'_2)a(q'_1) | \alpha \rangle \\ = |\alpha|^4 C^*(q_1)C^*(q_2)C(q'_2)C(q'_1) \end{aligned} \quad (20b)$$

In the detection plane, the first- and second-order correlation functions are calculated as

$$G^{(1)}(x_1, x_2) = |\alpha|^2 V^*(x_1)V(x_2) \quad (21a)$$

$$G^{(2)}(x_1, x_2) = |\alpha|^4 V^*(x_1)V^*(x_2)V(x_2)V(x_1) \quad (21b)$$

where

$$V(x) = \sqrt{\frac{k}{2\pi f}} \int \tilde{T}\left(\frac{kx}{f} - q\right) C(q) dq \quad (22)$$

The separability of spatial variables in the correlation functions Eqs. (21a) and (21b) verifies perfect coherence of the field, and it gives

$$G^{(2)}(x_1, x_2) = G^{(1)}(x_1, x_1)G^{(1)}(x_2, x_2) \quad (23)$$

The second-order interference consisting of the two first-order interference patterns can be factorized in terms of spatial positions. This feature is equivalent to the interference of the two independent photons $|\Psi\rangle_{SS}$ [see Eq. (13a)].

In the plane wave limit, the angular spectrum $C(q) = \delta(q)$, then we obtain $V(x) \propto \tilde{T}(kx/f)$, which indicates an ideal fringe pattern. For the coherent Gaussian beam that the angular spectrum is given by $|C(q)|^2 = (\sqrt{2\pi}w)^{-1} \exp[-q^2/(2w^2)]$, the first-order interference patterns related to the bandwidth of the Gaussian spectrum is plotted in Fig. 8(a). The fringe visibility is perfect and irrelevant to the bandwidth, that is, the angular spectrum of the coherent field does not degrade the coherence. In addition, as the bandwidth is increased, the fringe envelope is extended while the intensity drops rapidly. (The latter is not shown in the plot.)

According to Eq. (23), the second-order interference $G^{(2)}(x, x)$ has the same fringe period as the first-order one. Instead, if two independent modes of coherent beams illuminate the double-slit, Eq. (23) is replaced by

$$G^{(2)}(x_1, x_2) = G_H^{(1)}(x_1, x_1)G_V^{(1)}(x_2, x_2) \quad (24)$$

where the subscripts H and V designate two different modes, for instance, two orthogonally polarized modes. Assume that the two polarized beams are plane-wave with the same wavelength and incident upon the double-slit with a fixed angle, their angular spectra are $C_H(q) = \delta(q - Q_H)$ and $C_V(q) = \delta(q - Q_V)$. The second-order interference is thus written as

$$\begin{aligned} G^{(2)}(x_1, x_2) &\sim \cos^2\left[\left(\frac{kx_1}{f} - Q_H\right)\frac{d}{2}\right] \\ &\quad \cdot \cos^2\left[\left(\frac{kx_2}{f} - Q_V\right)\frac{d}{2}\right] \\ &= \frac{1}{4} \left\{ \cos\left[\left(\frac{k(x_1 + x_2)}{f} - (Q_H + Q_V)\right)\frac{d}{2}\right] \right. \\ &\quad \left. + \cos\left[\left(\frac{k(x_1 - x_2)}{f} - (Q_H - Q_V)\right)\frac{d}{2}\right] \right\}^2 \end{aligned} \quad (25)$$

where the envelope part has been neglected. By appropriately setting the incident angles, we obtain

$$G^{(2)}(x, x) \sim \frac{1}{4} \cos^2 \left[\left(\frac{k(2x)}{f} - (Q_H + Q_V) \right) \frac{d}{2} \right] \quad (26a)$$

when $(Q_H - Q_V)d = \pi$

$$G^{(2)}(x, -x) \sim \frac{1}{4} \cos^2 \left[\left(\frac{k(2x)}{f} - (Q_H - Q_V) \right) \frac{d}{2} \right]$$

when $(Q_H + Q_V)d = \pi$.

$$(26b) \quad |\Phi\rangle_j = \int_{-\infty}^{\infty} dq C_j(q) a^\dagger(q) |0\rangle, \quad j = 1, 2 \quad (30)$$

The fringes described by Eq. (26) have a half period of that for the first-order interference pattern. This scheme has been experimentally demonstrated [40].

Although the physics of this scheme is trivial, it tells us that the super-resolution of the fringe can be readily carried out with coherent beams. Moreover, there were other proposals using nonlinear optical processes to realize the super-resolution patterns [41,42]. But all of these schemes are different in essence from the second-order interference of both quantum entangled and classical correlated sources according to whether the first-order interference exists or not.

4.2 Quantum two-photon state source

A two-photon wavepacket consists of two photons, which are assumed to be monochromatic with the same wavelength. The two photons can be orthogonally or similarly polarized. The former has been discussed by Cao et al. [25], and here we focus on the latter.

A two-photon wavepacket containing two same polarized photons is written as

$$|\psi\rangle = \int_{\Sigma} dq_1 dq_2 C(q_1, q_2) a^\dagger(q_1) a^\dagger(q_2) |0\rangle \quad (27)$$

Since $a^\dagger(q_1) a^\dagger(q_2) |0\rangle$ and $a^\dagger(q_2) a^\dagger(q_1) |0\rangle$ denote the same state, the above integral is taken over a half plane Σ of the space (q_1, q_2) divided by the diagonal $q_1 = q_2$. We may extend the spectrum $C(q_1, q_2)$ to the whole space (q_1, q_2) by setting the symmetric condition $C(q_1, q_2) = C(q_2, q_1)$, and state (27) can be rewritten as

$$|\psi\rangle = \frac{1}{\sqrt{2}} \int_{-\infty}^{\infty} dq_1 \int_{-\infty}^{\infty} dq_2 C(q_1, q_2) a^\dagger(q_1) a^\dagger(q_2) |0\rangle \quad (28)$$

The state normalization gives

$$\begin{aligned} & \int_{-\infty}^{\infty} dq_1 \int_{-\infty}^{\infty} dq_2 C^*(q_1, q_2) C(q_1, q_2) \\ &= 2 \int_{\Sigma} dq_1 dq_2 C^*(q_1, q_2) C(q_1, q_2) = 1 \end{aligned} \quad (29)$$

If the two-photon wavepacket consists of two independent single-photon wavepackets

the unentangled two-photon state is thus given by

$$\begin{aligned} |\Psi\rangle_{SS} &= |\Phi\rangle_1 \otimes |\Phi\rangle_2 \\ &= \int_{-\infty}^{\infty} dq_1 \int_{-\infty}^{\infty} dq_2 C_1(q_1) C_2(q_2) a^\dagger(q_1) a^\dagger(q_2) |0\rangle \end{aligned} \quad (31)$$

where $C_j(q)$ is the single-photon angular spectrum satisfying

$$\int_{-\infty}^{\infty} C_j^*(q) C_j(q) dq = 1 \quad (32)$$

Since $C_1(q_1) C_2(q_2)$ and $C_1(q_2) C_2(q_1)$ are the amplitudes for the same state and can be added together, we may define a two-photon spectrum

$$C_{SS}(q_1, q_2) \equiv \frac{A}{2} [C_1(q_1) C_2(q_2) + C_1(q_2) C_2(q_1)] \quad (33)$$

which is symmetric by exchanging q_1 and q_2 . The unentangled two-photon state (31) can be equivalently expressed by Eq. (27) or Eq. (28) with the spectrum $C_{SS}(q_1, q_2)$. The normalization conditions (29) and (32) give

$$|A|^2 = \frac{2}{1 + |\beta|^2} \quad (34a)$$

$$\beta = \int_{-\infty}^{\infty} C_1^*(q) C_2(q) dq \quad (34b)$$

where β measures the overlap between the two single-photon wavepackets. For two degenerate wavepackets, i.e., $C_1(q) = C_2(q)$, it has $\beta = 1$ and $|A|^2 = 1$. However, for two orthogonal wavepackets, it has $\beta = 0$ and $|A|^2 = 2$.

For the sake of comparison, we show the first-order correlation for the single-photon wavepacket (30)

$$\langle \Phi | a^\dagger(q_1) a(q_2) | \Phi \rangle = C^*(q_1) C(q_2) \quad (35a)$$

$$G^{(1)}(x_1, x_2) = V^*(x_1) V(x_2) \quad (35b)$$

where $V(x)$ has been defined by Eq. (22). The first-order correlation and interference of a single photon are the same as the coherent field.

We now turn to the two-photon wavepacket described by Eq. (28). The first- and second-order correlation functions are obtained as

$$\langle \Psi | a^\dagger(q_1) a(q_2) | \Psi \rangle = \int C^*(q, q_1) C(q, q_2) dq \quad (36a)$$

$$\langle \Psi | a^\dagger(q_1) a^\dagger(q_2) a(q'_2) a(q'_1) | \Psi \rangle = C^*(q_1, q_2) C(q'_1, q'_2) \quad (36b)$$

Substituting Eqs. (36a) and (36b) into Eqs. (19a) and (19b), we obtain the corresponding correlation functions in the detection plane

$$G^{(1)}(x_1, x_2) = \frac{k}{2\pi f} \int \tilde{T}^* \left(\frac{kx_1}{f} - q_1 \right) \tilde{T} \left(\frac{kx_2}{f} - q_2 \right) C^*(q, q_1) C(q, q_2) dq dq_1 dq_2 \quad (37a)$$

$$G^{(2)}(x_1, x_2) = \left(\frac{k}{2\pi f} \right)^2 \left| \int \tilde{T} \left(\frac{kx_1}{f} - q_1 \right) \tilde{T} \left(\frac{kx_2}{f} - q_2 \right) C(q_1, q_2) dq_1 dq_2 \right|^2 \quad (37b)$$

In the following, we show three examples:

- (i) Two-photon wavepacket with the maximum entanglement $C(q_1, q_2) = \delta(q_1 + q_2)$. The first- and second-order correlation functions (36a) and (36b) can be evaluated as

$$\langle \Psi | a^\dagger(q_1) a(q_2) | \Psi \rangle = \delta(q_1 - q_2) \quad (38a)$$

$$\langle \Psi | a^\dagger(q_1) a^\dagger(q_2) a(q'_2) a(q'_1) | \Psi \rangle = \delta(q_1 + q_2) \delta(q'_1 + q'_2) \quad (38b)$$

Equation (38a) implies incoherence since each single photon of entangled photon pair is in a statistical mixture of states with different transverse wavevectors. Considering $|T(x)|^2 = T(x)$, we can calculate the integrals

$$\int \tilde{T}^* \left(\frac{kx_1}{f} \pm q \right) \tilde{T} \left(\frac{kx_2}{f} \pm q \right) dq = \sqrt{2\pi} \tilde{T} \left[\frac{k}{f} (x_2 - x_1) \right] \quad (39a)$$

$$\int \tilde{T}^* \left(\frac{kx_1}{f} \pm q \right) \tilde{T} \left(\frac{kx_2}{f} \mp q \right) dq = \sqrt{2\pi} \tilde{T} \left[\frac{k}{f} (x_2 + x_1) \right] \quad (39b)$$

The correlation functions are obtained as

$$G^{(1)}(x_1, x_2) = \frac{k}{2\pi f} \sqrt{2\pi} \tilde{T} \left[\frac{k}{f} (x_2 - x_1) \right] \quad (40a)$$

$$G^{(2)}(x_1, x_2) = \left(\frac{k}{2\pi f} \right)^2 2\pi \left| \tilde{T} \left[\frac{k}{f} (x_2 + x_1) \right] \right|^2 \quad (40b)$$

The first-order double-slit interference disappears, that is, $G^{(1)}(x, x) \propto \tilde{T}[0]$. However, the second-order double-slit interference shows the sub-wavelength feature owing to $G^{(2)}(x, x) \propto \left| \tilde{T} \left[\frac{k}{f} (2x) \right] \right|^2$. We notice that the same feature exists in the two-photon interference scheme using a beamsplitter [16], where for the two-photon entangled state the second-order interference shows sub-wavelength fringe while the first-order interference does not occur.

- (ii) Entangled beams produced in spontaneous parametric down-conversion (SPDC)

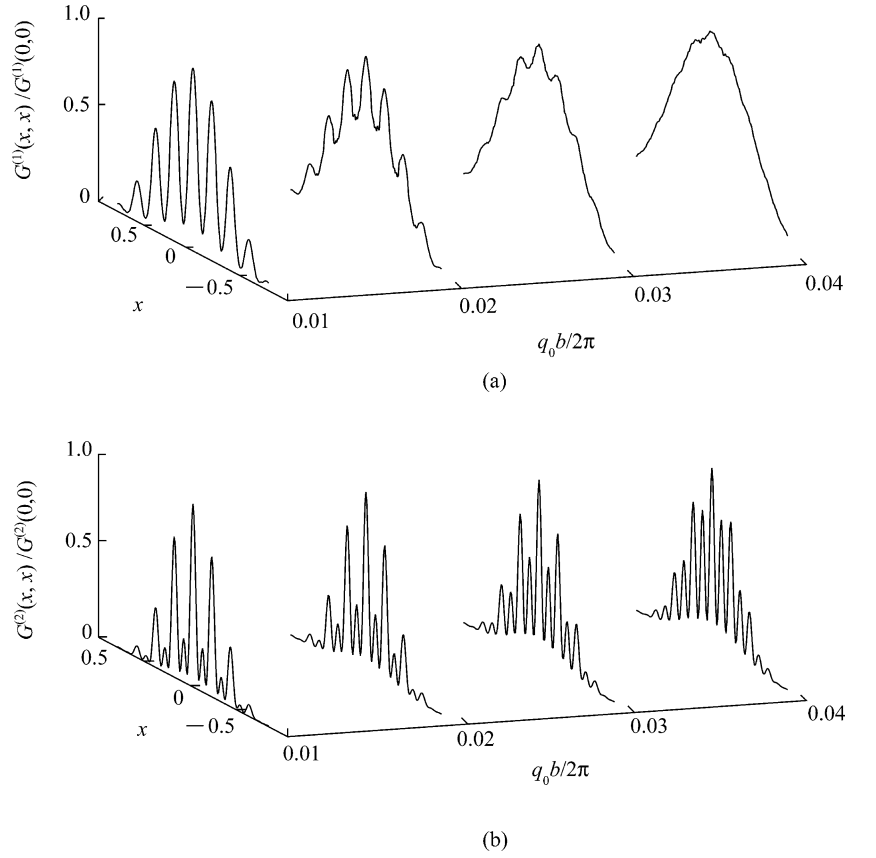
The first- and second-order correlation functions for the spontaneous parametric beams produced in type-I crystal are written as [25]

$$\langle a^\dagger(q_1) a(q_2) \rangle = |V(q)|^2 \delta(q_1 - q_2), \quad (41a)$$

$$\begin{aligned} \langle a^\dagger(q_1) a^\dagger(q_2) a(q'_2) a(q'_1) \rangle &= V^*(q_1) U^*(q_2) V(q'_2) U(q'_1) \\ &\quad \delta(q_1 + q_2) \delta(q'_1 + q'_2) + V^*(q_1) \\ &\quad V^*(q_2) V(q'_2) \times V(q'_1) [\delta(q_1 - q'_1) \\ &\quad \delta(q_2 - q'_2) + \delta(q_1 - q'_2) \delta(q_2 - q'_1)] \end{aligned} \quad (41b)$$

where U and V are the transfer coefficients. Equation (41a) corresponds to the first-order spectral correlation of a classical stochastic variable which satisfies the Wiener-Khintchine theorem [see Eq. (44) below].

Fig. 7 (a) First-order interference patterns and (b) second-order interference patterns vs the normalized bandwidths $q_0 b / (2\pi)$ of SPDC process, where the coupling parameter $g = 0.4$



However, the second term in Eq. (41b) describes a classical thermal correlation (see Eq. (45) below). In the weak coupling case when $|U| \gg |V|$, the classical correlation term can be omitted, and Eqs. (41a) and (41b) display the similar correlation as Eqs. (38a) and (38b) for the two-photon entangled state. Using Eqs. (41a) and (41b) and Eqs. (19a) and (19b), we calculate the first- and second-order interference patterns and plot them in Fig. 7. As the bandwidth of the transfer coefficients is increased, the first-order interference fringe disappears while the second-order interference fringe exhibits the sub-wavelength characteristic.

- (iii) Unentangled two-photon wavepacket $C_{SS}(q_1, q_2)$
Substituting Eq. (33) into Eqs. (37a) and (37b), we obtain

$$G^{(1)}(x_1, x_2) = \frac{|A|^2}{4} \{ V_1^*(x_1) V_1(x_2) + V_2^*(x_1) V_2(x_2) + \beta V_1^*(x_1) V_2(x_2) + \beta^* V_2^*(x_1) V_1(x_2) \} \quad (42a)$$

$$G^{(2)}(x_1, x_2) = \frac{|A|^2}{4} |V_1(x_1) V_2(x_2) + V_2(x_1) V_1(x_2)|^2 \quad (42b)$$

where $V_j(x)$ is defined by Eq. (22). The first-order double-slit interference pattern is thus

$$G^{(1)}(x, x) = \frac{|A|^2}{4} \{ |V_1(x)|^2 + |V_2(x)|^2 + [\beta V_1^*(x) V_2(x) + \text{c.c.}] \} \quad (43)$$

This means that each single-photon wavepacket generates its own pattern while the overlap between the two wavepackets, described by β , brings about the “secondary interference” between the two patterns. This comes from the indistinguishability of two photons. However, the second-order interference pattern is irrelevant to the overlap of wavepackets.

If two single-photon wavepackets are identical, that is, $V_1(x) = V_2(x) \equiv V(x)$ and $\beta = |A|^2 = 1$, we obtain $G^{(1)}(x_1, x_2) = V^*(x_1) V(x_2)$ and $G^{(2)}(x_1, x_2) = |V(x_1) V(x_2)|^2 = G^{(1)}(x_1, x_1) G^{(1)}(x_2, x_2)$. Therefore, the two independent degenerate single-photon wavepackets exhibit the same interference behaviors as that for the coherent field.

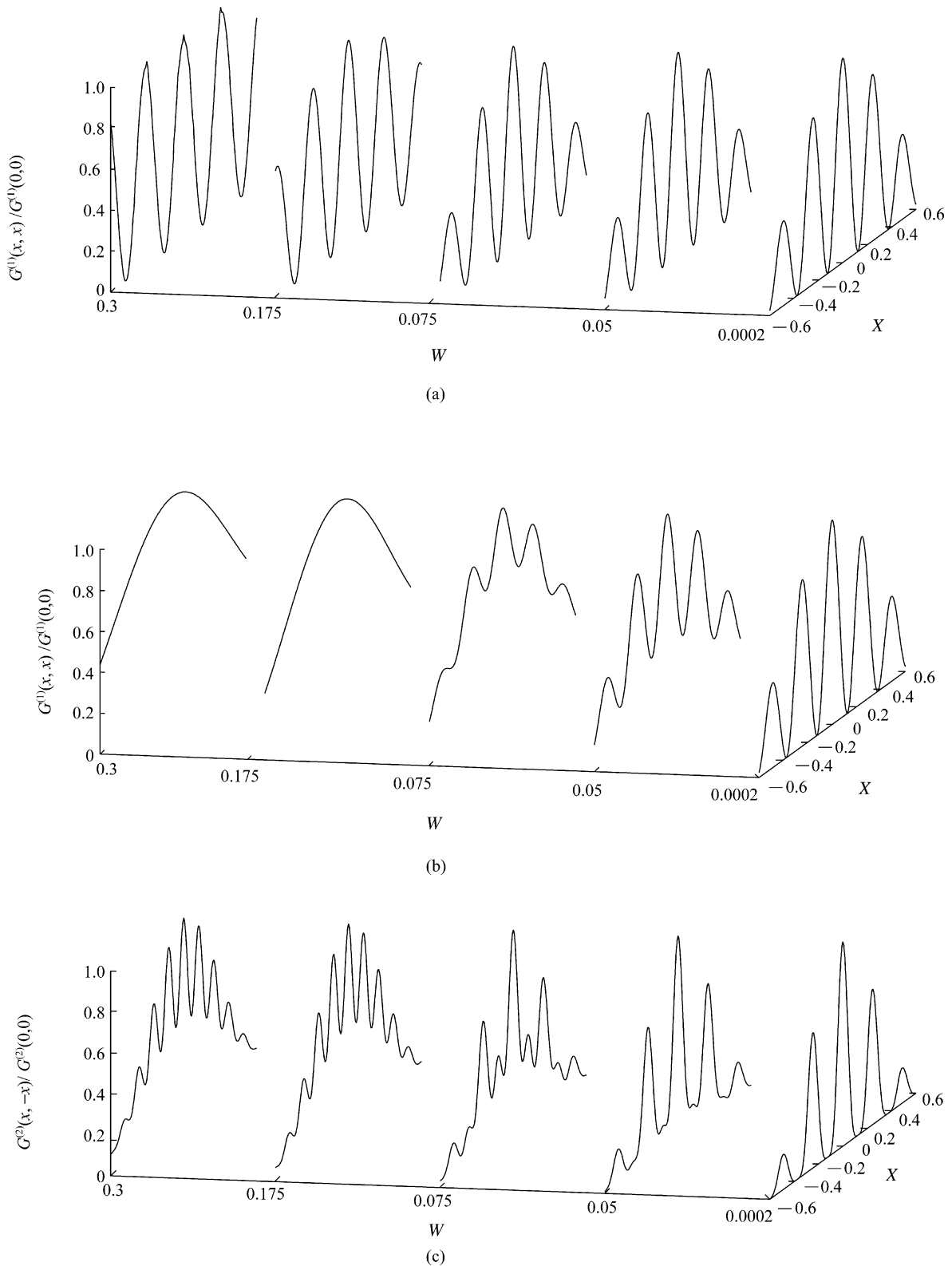


Fig. 8 (a) First-order interference patterns of coherent fields for different normalized bandwidths $W = wb/(2\pi)$ of the Gaussian angular spectrum. (b) First-order interference patterns and (c) second-order interference patterns of thermal light for different normalized

bandwidths W of the Gaussian power spectrum. The X -axis $X = xkb/(2\pi f)$ is the normalized position in the detection plane and the double-slit parameter is taken to be $d = 4b$

4.3 Classical thermal light source

Let us now consider a classical thermal light source. We assume a monochromatic plane wave $E_0 \exp[i(kz - \omega t)]$ illuminating a material containing disordered scattering centers. After scattering, the field is written as $E(x, z, t) = \int E(q) \exp[i(qx + k_z z - \omega t)] dq$, where q is the transverse wavevector introduced by the random scattering and satisfies $q^2 + k_z^2 = k^2$. Hence, $E(q)$ is a stochastic variable obeying Gaussian statistics. If $q \ll k$, the scattered field can be approximately written as $E(x, z, t) = A(x) \exp[i(kz - \omega t)]$, where $A(x) = \int E(q) \exp[iqx] dq$ is the slowly varying envelope. As a result, we have defined a monochromatic pseudo-thermal

light random in both strength and propagation direction. According to the Wiener–Khinchine theorem, the first-order spectral correlation must satisfy

$$\langle E^*(q)E(q') \rangle = S(q)\delta(q - q') \quad (44)$$

where $S(q)$ is the power spectrum of the spatial frequency.

For any random variable with Gaussian statistics, all high-order correlations can be expressed in terms of the first-order ones [43]. Hence, the second-order spectral correlation of thermal light can be written as

$$\begin{aligned} \langle E^*(q_1)E^*(q_2)E(q'_2)E(q'_1) \rangle &= \langle E^*(q_1)E(q'_1) \rangle \langle E^*(q_2)E(q'_2) \rangle + \langle E^*(q_1)E(q'_2) \rangle \langle E^*(q_2)E(q'_1) \rangle \\ &= S(q_1)S(q_2)[\delta(q_1 - q'_1)\delta(q_2 - q'_2) + \delta(q_1 - q'_2)\delta(q_2 - q'_1)]. \end{aligned} \quad (45)$$

Combining the correlation nature in Gaussian statistics with the Wiener–Khinchine theorem, Eq. (45) implies spatial intensity correlation. When the thermal light is split into two beams at a beam splitter, the two output beams are spatially correlated. This is the origin of the correlated imaging and interference for the classical thermal source. As a matter of fact, there is no such correlation in any coherent beam, so the correlated imaging can not occur. However, in the case of two-photon entanglement, the field correlation exists within the same spatial frequency components, as shown in Eq. (36b). In particular, in the spontaneous parametric down-conversion process, the entanglement occurs in photon pairs satisfying the momentum conservation, and the second-order correlation is given by Eq. (38b).

Substituting Eqs. (44) and (45) into Eqs. (19a) and (19b), we obtain

$$G^{(1)}(x_1, x_2) = \frac{k}{2\pi f} \int \tilde{T}^* \left(\frac{kx_1}{f} - q \right) \tilde{T} \left(\frac{kx_2}{f} - q \right) S(q) dq \quad (46a)$$

$$G^{(2)}(x_1, x_2) = G^{(1)}(x_1, x_1)G^{(1)}(x_2, x_2) + |G^{(1)}(x_1, x_2)|^2 \quad (46b)$$

The interference patterns depend on the bandwidth of spectrum $S(q)$ with respect to the double-slit parameter, characterized by $1/b$. In the narrow bandwidth limit, $S(q) \rightarrow \delta(q)$, the correlation functions become the same as the coherent field, since, in this case, the disorder is trivial. However, in the broadband limit when $S(q) \rightarrow S_0$, Eqs. (46a) and (46b) are written as

$$G^{(1)}(x_1, x_2) = \frac{k}{2\pi f} \sqrt{2\pi} S_0 \tilde{T} \left[\frac{k}{f} (x_2 - x_1) \right] \quad (47a)$$

$$G^{(2)}(x_1, x_2) = \left(\frac{k}{2\pi f} \right)^2 2\pi S_0^2 \left\{ \tilde{T}^2(0) + \left| \tilde{T} \left[\frac{k}{f} (x_1 - x_2) \right] \right|^2 \right\} \quad (47b)$$

where Eq. (39a) is applied. The first-order correlation function is the same as that for the two-photon entangled state, given by Eq. (40a), so that the first-order interference disappears, i.e., $G^{(1)}(x, x) \propto \tilde{T}[0]$. This is in accordance with the conventional understanding that the disorder in spatial wavevectors washes out the interference pattern. However, the interference pattern can be extracted through joint-intensity measurement. For example, when two detectors in the joint-intensity measurement are scanned in the opposite directions with respect to a position x_0 , i.e. $x_1 = x_0 + x$ and $x_2 = x_0 - x$, we obtain $G^{(2)}(x_1, x_2) \propto \tilde{T}^2(0) + \left| \tilde{T} \left[\frac{k}{f} (2x) \right] \right|^2$. The interference pattern is the same as that for the entangled photon pair in the two-photon detection, except that the background accompanies the fringe for the thermal light, causing the maximum visibility of 33.3%, whereas for the entangled two-photon state the fringe has perfect visibility.

In the general case, we set the Gaussian power spectrum to be $S(q) = (\sqrt{2\pi}w)^{-1} \exp[-q^2/(2w^2)]$. Fig. 8(b)–(c) shows the first- and second-order interference patterns for the different normalized bandwidths $W = wb/(2\pi)$, respectively. At very small bandwidth, both the first- and second-order interference patterns show the same fringes as that for the coherent beam. As the bandwidth increases, the first-order interference disappears and the second-order interference shows half of the fringe period for the first-order one.

5 Conclusions

In summary, we have shown the second-order double-slit interference for an incoherent light source both experimentally and theoretically. The theoretical description, which is carried out in contrast with coherent light and two-photon state sources, demonstrates that this effect is the double-slit interference version of the Hanbury–Brown and Twiss effect. Therefore, we gain new knowledge about the interference effect of incoherent light.

Both the first- and second-order double-slit interference reflect the statistics and spatial correlation of optical fields. For the coherent field and the two independent photons, the second-order interference is the product of two first-order ones, resulting in the decorrelation of spatial variables. However, for both the two-photon entangled state and the thermal light, the second-order interference appears in the form that two spatial positions are correlated while the first-order interference disappears. In spite of the similarity of the effects for both sources, we may conclude different physics for them: the quantum coherent interference for the two-photon entangled source and the Hanbury–Brown and Twiss-type interference for the incoherent light source.

Acknowledgements This study was supported by the National Fundamental Research Program of China Project (No. 2001CB3093 10), and the National Natural Science Foundation of China Project (Nos. 60278021, 10074008 and 10574015). One of the authors, WANG Kai-ge, acknowledges the financial support of the Abdus Salam International Centre for Theoretical Physics (ICTP) under the Associate Program.

References

1. Feynman R.-P., Leighton R.-B. and Sands M., *The Feynman Lectures on Physics*, Vol. 3, Chap. 1, Reading, MA: Addison-Wesley, 1965
2. Born M. and Wolf E., *Principles of Optics* (seventh edn.), Chap. 10, Cambridge, England: Cambridge University Press, 1999
3. Ribeiro P.-H.-S., Pádua S., Machado da Silva J.-C. and Barbosa G.-A., *Phys. Rev. A*, 1994, 49: 4176
4. Strekalov D.-V., Sergienko A.-V., Klyshko D.-N. and Shih Y.-H., *Phys. Rev. Lett.*, 1995, 74: 3600; Pittman T.-B., Shih Y.-H., Strekalov D.-V. and Sergienko A.-V., *Phys. Rev. A*, 1995, 52, R3429
5. Souto Ribeiro P.-H. and Barbosa G.-A., *Phys. Rev. A*, 1996, 54: 3489
6. Barbosa G.-A., *Phys. Rev. A*, 1996, 54: 4473
7. Fonseca E.-J.-S., Monken C.-H., Pádua S. and Barbosa G.-A., *Phys. Rev. A*, 1999, 59: 1608
8. Fonseca E.-J.-S., Souto Ribeiro P.-H., Pádua S. and Monken C.-H., *Phys. Rev. A*, 1999, 60: 1530
9. Fonseca E.-J.-S., Machado da Silva, J.-C., Monken C.-H. and Pádua S., *Phys. Rev. A*, 2000, 61: 023801
10. Saleh B.-E.-A., Abouraddy A.-F., Sergienko A.-V. and Teich M.-C., *Phys. Rev. A*, 2000, 62: 043816
11. Abouraddy A.-F., Saleh B.-E.-A., Sergienko A.-V. and Teich M.-C., *Phys. Rev. Lett.*, 2001, 87: 123602
12. Abouraddy A.-F., Nasr M.-B., Saleh B.-E.-A., Sergienko A.-V. and Teich M.-C., *Phys. Rev. A*, 2001, 63: 063803
13. Gatti A., Brambilla E. and Lugiato L.-A., *Phys. Rev. Lett.*, 2003, 90: 133603
14. Jacobson J., Björk G., Chuang I. and Yamamoto Y., *Phys. Rev. Lett.*, 1995, 74: 4835
15. Fonseca E.-J.-S., Monken C.-H. and Pádua S., *Phys. Rev. Lett.*, 1999, 82: 2868
16. Boto A.-N., Kok P., Abrams D.-S., Braunstein S.-L., Williams C.-P. and Dowling J.P., *Phys. Rev. Lett.*, 2000, 85: 2733
17. D'Angelo M., Chekhova M.-V. and Shih Y., *Phys. Rev. Lett.*, 2001, 87: 013602
18. Fonseca E.-J.-S., Paulini Z., Nussenzveig P., Monken C.-H. and Pádua S., *Phys. Rev. A*, 2001, 63: 043819
19. Nagasako E.-M., Bentley S.-J., Boyd R.-W. and Agarwal G.-S., *Phys. Rev. A*, 2001, 64: 043802
20. Björk G., Sánchez-Soto L.-L. and Söderholm J., *Phys. Rev. Lett.*, 2001, 86: 4516; *Phys. Rev. A*, 2001, 64: 013811
21. Edamatsu K., Shimizu R. and Itoh T., *Phys. Rev. Lett.*, 2002, 89: 213601
22. Steuernagel O., *Phys. Rev. A*, 2002, 65: 033820
23. Shimizu R., Edamatsu K. and Itoh T., *Phys. Rev. A*, 2003, 67: 041805(R)
24. Cao D.-Zh. and Wang K., *Phys. Lett. A*, 2004, 333: 23
25. Cao D.-Zh., Li Zh., Zhai Y.-H. and Wang K., *Eur. Phys. J.D.*, 2005, 33: 137
26. Klyshko D.-N., *Phys. Lett. A*, 1988, 128: 133; 1988, 132: 299
27. Bennink R.-S., Bentley S.-J. and Boyd R.-W., *Phys. Rev. Lett.*, 2002, 89: 113601; Bennink R. S., Bentley S. J., Boyd R. W., Howell J.-C., *Phys. Rev. Lett.*, 2004, 92: 033601
28. D'Angelo M. and Shih Y., *quant-ph/0302146*
29. D'Angelo M., Kim Y.-H., Kulik S.-P. and Shih Y., *Phys. Rev. Lett.*, 2004, 92: 233601
30. Gatti A., Brambilla E., Bache M. and Lugiato L.-A., *Phys. Rev. Lett.*, 2004, 93: 093602; *Phys. Rev. A*, 2004, 70: 013802
31. Cheng J. and Han Sh., *Phys. Rev. Lett.*, 2004, 92: 093903
32. Wang K. and Cao D.-Zh., *Phys. Rev. A*, 2004, 70: 041801(R)
33. Cao D.-Zh. and Wang K., *Phys. Rev. A*, 2005, 71: 013801
34. Cai Y. and Zhu Sh., *Opt. Lett.*, 2004, 29: 2716; *Phys. Rev. E*, 2005, 71: 056607
35. Xiong J., Cao D.-Zh., Huang F., Li H.-G., Sun X.-J. and Wang K., *Phys. Rev. Lett.*, 2005, 94: 173601
36. Ferri F., Magatti D., Gatti A., Bache M., Brambilla E. and Lugiato L.-A., *Phys. Rev. Lett.*, 2005, 94: 183602
37. Scarcelli G., Valencia A. and Shih Y., *Phys. Rev. A*, 2004, 70: 051802(R); *Europhys. Lett.*, 2004, 68: 618; Valencia A., Scarcelli G., D'Angelo M. and Shih Y. *Phys. Rev. Lett.*, 2005, 94: 063601
38. Zhang D., Zhai Y.-H., Wu L.-A. and Chen X.-H., *Opt. Lett.* 2005, 30: 2354
39. Hanbury R. and Twiss R.-Q., *Nature*, 1956, 177: 27; 1956, 178: 1447
40. Jun Xiong, Feng Huang, Dezhong Cao, Hongguo Li, Xujuan Sun and Kaige Wang, *Chin. Phys. Lett.*, 2005, 22: 2824
41. Yablonovitch E. and Vrijen R.-B., *Opt. Eng.*, 1999, 38: 334
42. Bentley S.-J. and Boyd R.-W., *Opt. Express*, 2004, 12: 5735
43. Mandel L. and Wolf E., *Optical Coherence and Quantum Optics*, Chap. 1, Cambridge: Cambridge University Press, 1995